

---

# FreqKV: Frequency Domain Key-Value Compression for Efficient Context Window Extension

---

Jushi Kai<sup>1</sup>, Boyi Zeng<sup>1</sup>, Yixuan Wang<sup>1</sup>, Haoli Bai<sup>2</sup>, Bo Jiang<sup>3</sup>, Zhouhan Lin<sup>1\*</sup>

<sup>1</sup>LUMIA Lab, Shanghai Jiao Tong University

<sup>2</sup>Huawei Noah's Ark Lab

<sup>3</sup>Shanghai Jiao Tong University

{json.kai, boyizeng, luckywang, bjiang}@sjtu.edu.cn

baihaoli@huawei.com, lin.zhouhan@gmail.com

## Abstract

Extending the context window in large language models (LLMs) is essential for applications involving long-form content generation. However, the linear increase in key-value (KV) cache memory requirements and the quadratic complexity of self-attention with respect to sequence length present significant challenges during fine-tuning and inference. Existing methods suffer from performance degradation when extending to longer contexts. In this work, we introduce a novel context extension method that optimizes both fine-tuning and inference efficiency. Our method exploits a key observation: in the frequency domain, the energy distribution of the KV cache is primarily concentrated in low-frequency components. By filtering out the high-frequency components, the KV cache can be effectively compressed with minimal information loss. Building on this insight, we propose an efficient compression technique, FreqKV, that iteratively compresses the increasing KV cache to a fixed size in the frequency domain, applicable to both fine-tuning and inference. FreqKV introduces no additional parameters or architectural modifications. With minimal fine-tuning, LLMs can learn to leverage the limited cache that is compressed in the frequency domain and extend the context window efficiently. Experiments on various long context language modeling and understanding tasks demonstrate the efficiency and efficacy of the proposed method.

## 1 Introduction

Large language models (LLMs) typically have a limited size of context window, which is pre-defined during the pre-training process. However, it is inevitable for LLMs to process sequences that exceed the preset context size. LLMs struggle to maintain their performance when generalized to longer contexts. Additionally, the computation cost of the self-attention mechanism [23] grows quadratically with the context length, meaning that doubling the context window results in a fourfold increase in the computational cost of attention modules.

For efficiency, existing efforts aim to compress the key-value (KV) cache for long contexts during inference. They evict [26, 17] or merge [29, 24] KV states of less important tokens following certain rules. They use attention scores to measure the importance and approximate the original full attention. However, while these methods provide an approximation of full computation on existing tokens through different strategies, they can not fully prevent performance degradation when decoding future tokens.

---

\*Corresponding Author.

Recent studies propose to fine-tune LLMs to longer contexts to extend the context window. LongLoRA [7] trains LLMs using shifted sparse attention. Despite training efficiency, their sparse attention fails to be applied during inference, and they still require the original attention on the full sequence. Concurrently, LoCoCo [5] and Activation Beacon [28] introduce additional modules to compress KV states. They incorporate the fine-tuned compressing pattern into the decoding procedure of LLMs.

In the field of computer vision, studies have shown that low-frequency channels are more important for convolutional neural networks (CNNs) [27]. Moreover, Fourier Transformer [13] discards the high-frequency parts of the contexts and downsample the hidden states in the encoders. Inspired by these works, we seek to compress KV states in the frequency domain without the need for additional compression modules in decoder-only LLMs. We transform key states and value states in LLaMA-2-7b [22] from the time domain to the frequency domain for power spectrum analysis. As shown in Figure 1, the energy distribution increasingly concentrates on low-frequency components as the computation process progresses along the decoder layers. It suggests that high-frequency components, which occupy less energy and contribute less to the overall information, can be discarded without much performance loss, thereby enhancing computational efficiency.

In this paper, we introduce FreqKV, an efficient context extension method that iteratively compresses key-value states in the frequency domain. Compression is triggered only when the KV cache reaches the predefined context window size. During each compression step, the low-frequency components of the KV states are preserved at a specified retaining ratio. Subsequent tokens are appended to the compressed cache until it is filled again. This ensures that the cached KV states that each query token can attend to is limited below the context window size. To reduce memory and computational costs, the compressed cache will be further compressed together with the incoming tokens. This iterative compression mechanism leads to an increased compression level of the earlier contexts as the sequence length grows. Without introducing additional compression modules, LLMs could learn to utilize the compressed cache efficiently when extending to longer contexts. FreqKV demonstrates comparable performance to other methods that employ full KV cache or additional compressors in long context language modeling. Furthermore, experiments on downstream tasks indicate that FreqKV surpasses recently studied KV compression methods in long-context understanding.

## 2 Related Work

**KV Compression for LLMs.** To extend the context window of LLMs efficiently, researchers attempt to compress the KV cache as more tokens are fed into the model. One common approach is selective token eviction [26, 17, 6], where less significant tokens are discarded. Although the eviction strategies ensure that the size of KV cache involved in each decoding step does not exceed the predefined context window size, LLMs suffer from the permanent loss of the information associated with evicted tokens. To address this limitation, some researchers introduce cache merging techniques to approximate the original full attention of the existing contexts [29, 24, 25]. However, these inference methods often sacrifice performance for efficiency.

**Context Extension for LLMs.** Recent advancements in context extension for LLMs have focused on efficiently scaling models to handle longer input sequences without significantly increasing computational costs. LongLoRA [7] employs shifted sparse attention during the parameter-efficient fine-tuning. However, this sparse attention mechanism is not applicable during inference, necessitating a return to the original full attention post-training. Other techniques, such as LoCoCo [5], integrate convolutional operations into LLMs for compressing long contexts. They fine-tune the compression modules together with LLMs. Landmark attention [19] uses landmark tokens to retrieve previous input blocks. Similarly, Activation Beacon [28] introduces a special token to represent the previous context for compression. However, they need a copy of multi-head attention, which amounts to approximately 2B for 7B models. In contrast, our proposed method achieves context extension without introducing any additional parameters.

**Learning in the Frequency Domain.** Learning in the frequency domain is a well-established technique to compress images and accelerate CNNs [11]. It has been observed that CNNs are more sensitive to low-frequency channels than high-frequency channels [27]. These works have inspired efforts to process natural language. FNet [16] enhances the efficiency of Transformer encoder architectures by replacing the self-attention layers with the Fourier transform to serve the purpose

of mixing tokens. Additionally, Fourier Transformer [13] eliminates redundancies in the context through frequency domain processing within encoder architectures.

However, because of the auto-regressive nature, it remains unclear how to leverage frequency components for decoder-only Transformer, which is the main architecture of generative LLMs. To the best of our knowledge, FreqKV is the first work that explores compressing key-value states in the frequency domain for decoder-only LLMs.

### 3 Preliminaries

#### 3.1 Discrete Cosine Transform

The Discrete Cosine Transform (DCT) transforms a signal from the spatial domain (time or position) into the frequency domain. Several variants of the DCT exist, with DCT-II being the most common. For a real-value discrete signal  $\mathbf{X}_{0:N-1} = [x_0, \dots, x_{N-1}]$  of length  $N$ , it is defined as:

$$y_t = \alpha_t \sum_{n=0}^{N-1} x_n \cdot \cos \left[ \frac{\pi t(2n+1)}{2N} \right], \quad \alpha_t = \begin{cases} \sqrt{\frac{1}{N}} & \text{if } t = 0, \\ \sqrt{\frac{2}{N}} & \text{otherwise} \end{cases} \quad (1)$$

where  $t = 0, 1, \dots, N-1$ .  $\alpha_t$  is the normalization factor.

The time-domain signal  $\mathbf{X}_{0:N-1}$  can be recovered by applying the inverse DCT (IDCT) on the frequency components  $\mathbf{Y}_{0:N-1}$ :

$$x_n = \sum_{t=0}^{N-1} \alpha_t \cdot y_t \cdot \cos \left[ \frac{\pi t(2n+1)}{2N} \right]. \quad (2)$$

The frequency components are expressed as a combination of the original signals. The values can be computed using the Fast Fourier Transform (FFT) with a complexity of  $O(N \log N)$ . The amplitudes of frequency components are utilized in the power spectrum analysis to represent the energy or magnitude of components. The components of higher energy in the frequency domain indicate they are more informative [13].

#### 3.2 Self-Attention

For the incoming token  $x_N$ , the prefilled  $N$  tokens  $\mathbf{X}_{0:N-1}$  are utilized as the cache during decoding. Denote the hidden states of the  $N+1$  tokens input to a specific layer of LLMs as  $\mathbf{H}_{0:N} = [h_0, \dots, h_N]$ . The query, key and value states of  $x_N$  are computed as follows::

$$\mathbf{q}_N = \mathbf{h}_N \mathbf{W}^Q, \quad \mathbf{k}_N = \mathbf{h}_N \mathbf{W}^K, \quad \mathbf{v}_N = \mathbf{h}_N \mathbf{W}^V, \quad (3)$$

where  $\mathbf{W}^Q, \mathbf{W}^K, \mathbf{W}^V$  are the projection matrices for the query, key and value states, respectively. For simplicity, indices corresponding to layers and heads have been omitted.

The cached KV states for the previous  $N$  tokens  $\mathbf{X}_{0:N-1}$  are:

$$\mathbf{K}_{0:N-1} = \mathbf{H}_{0:N-1} \mathbf{W}^K, \quad \mathbf{V}_{0:N-1} = \mathbf{H}_{0:N-1} \mathbf{W}^V. \quad (4)$$

When calculating attention scores, the incoming token  $x_N$  attends to all cached KV states as well as to itself:

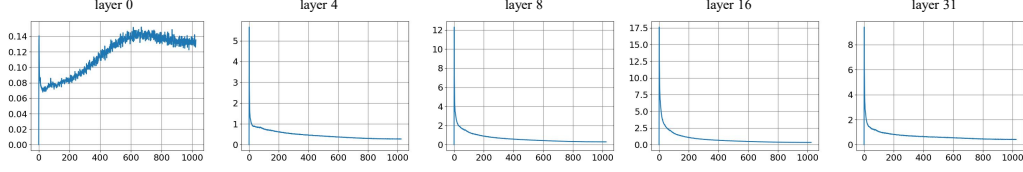
$$\mathcal{A}(N) = \text{Softmax} \left( \frac{\mathbf{q}_N [\mathbf{K}_{0:N-1} \oplus \mathbf{k}_N]^T}{\sqrt{d}} \right) \cdot [\mathbf{V}_{0:N-1} \oplus \mathbf{v}_N], \quad (5)$$

where  $d$  is the hidden dimension.  $\oplus$  means the concatenation of the KV cache and KV states of  $x_N$

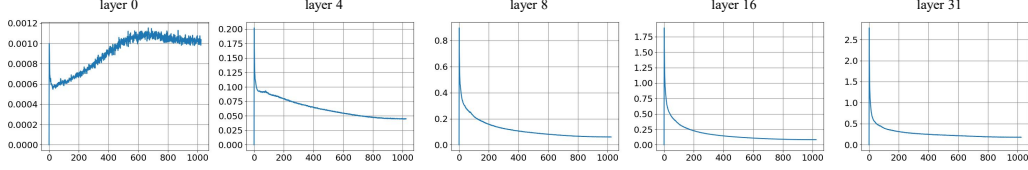
### 4 FreqKV

#### 4.1 Energy Concentration in the Frequency Domain

We transform key states and value states from the time domain, which is the sequence dimension, to the frequency domain. The average power spectrums in different decoder layers of LLaMA-2-7b are calculated and presented in Figure 1.



(a) The average power spectra of key states.



(b) The average power spectra of value states.

Figure 1: The average power spectra of key states and value states in different layers of LLaMA-2-7b. 1000 documents are sampled from CNN/Daily Mail [14]. We use DCT to transform key states and value states to the frequency domain, and average power spectrums over these samples and hidden dimensions.

The figure shows that the energy of key states and value states is increasingly concentrated in the low-frequency components. The distributions of their power spectrums are similar since they are projected from the same hidden states as shown in Equation 3. Although there is no obvious energy concentration in the frequency domain for the initial embeddings of natural languages in the first layer, the model tends to aggregate energy in the low-frequency components along the decoding procedure. The observation of energy concentration suggests that we could maintain low-frequency components and filter out high-frequency components which could be redundant. Head-wise analysis of the power spectrum is provided in Appendix A.

## 4.2 KV Compression in the Frequency Domain

We conduct DCT along the sequence dimension to transfer the KV cache to the frequency domain:

$$\mathbf{Y}_{0:N-1}^K = \text{DCT}(\mathbf{K}_{0:N-1}), \quad \mathbf{Y}_{0:N-1}^V = \text{DCT}(\mathbf{V}_{0:N-1}). \quad (6)$$

As observed in Figure 1, since the lower-frequency components are of higher magnitude and carry more information, we will retain them and remove higher-frequency components for compression. Given the retaining ratio  $\gamma$ , the retaining size is  $L = \gamma \cdot N$ .  $N - L$  high-frequency components are filtered out to reduce redundancy:

$$\tilde{\mathbf{Y}}_{0:L-1}^K = \mathbf{Y}_{0:N-1}^K[0:L-1], \quad \tilde{\mathbf{Y}}_{0:L-1}^V = \mathbf{Y}_{0:N-1}^V[0:L-1]. \quad (7)$$

Then we conduct IDCT along the frequency dimension to convert the compressed components back to the time dimension. It should be noted that the signals are normalized by the square root of the component number as shown in the formulas of DCT and IDCT. While DCT works on  $N$  time-domain signals, only  $L$  frequency-domain signals are processed by IDCT. The compressed states are amplified by  $\sqrt{\frac{N}{L}}$  during the transforms. Therefore, the compressed signals should be rescaled with the factor of  $\sqrt{\frac{L}{N}}$  to restore the original amplitude:

$$\tilde{\mathbf{K}}_{0:L-1}^{0:N-1} = \sqrt{\frac{L}{N}} \text{IDCT}(\tilde{\mathbf{Y}}_{0:L-1}^K), \quad \tilde{\mathbf{V}}_{0:L-1}^{0:N-1} = \sqrt{\frac{L}{N}} \text{IDCT}(\tilde{\mathbf{Y}}_{0:L-1}^V). \quad (8)$$

$\tilde{\mathbf{K}}_{0:L-1}^{0:N-1}$  and  $\tilde{\mathbf{V}}_{0:L-1}^{0:N-1}$  are the compressed KV cache of size  $L$  in the time domain. The superscript “ $0:N-1$ ” means that  $\tilde{\mathbf{K}}_{0:L-1}^{0:N-1}$  and  $\tilde{\mathbf{V}}_{0:L-1}^{0:N-1}$  are the compressed KV of the cached  $N$  tokens. The

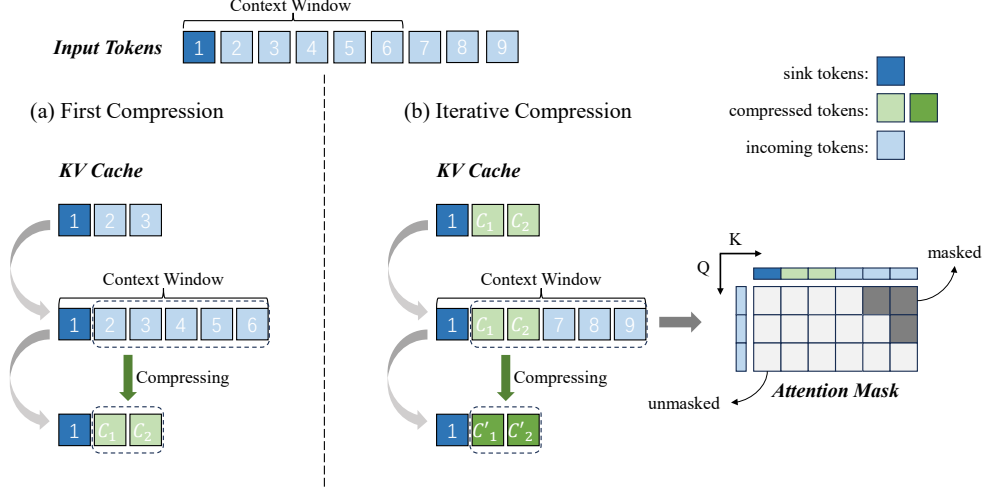


Figure 2: The illustration of our FreqKV. The KV cache will be compressed in an iterative manner as the cache reaches the context window size. Sink tokens remain uncompressed throughout the process. (a) The tokens after sink tokens will be compressed in the frequency domain and subsequent tokens will continue to get into the cache. (b) When the cache is filled again, the compressed tokens and incoming tokens will be compressed together. The compression is performed iteratively to extend the context window.

subscript “ $0:L-1$ ” means the retaining size is  $L$ . The incoming token  $x_N$  will attend to the compressed KV cache:

$$\tilde{A}(N, L) = \text{Softmax} \left( \frac{q_N [\tilde{K}_{0:L-1}^{0:N-1} \oplus k_N]^T}{\sqrt{d}} \right) \cdot [\tilde{V}_{0:L-1}^{0:N-1} \oplus v_N]. \quad (9)$$

### 4.3 Context Extension with the Compressed KV

When extending the context window, the memory requirement of KV cache increases linearly and the computation cost of the original full attention grows quadratically with the length. To limit the size of KV cache for each query token to attend below the context window size, we will compress KV cache in the frequency domain iteratively as the cache is filled. We illustrate our FreqKV in Figure 2.

For tokens within the context window, the standard attention will be conducted. For tokens out of the window, we will compress the cached KV states in the frequency domain. Because the retaining size  $L$  is smaller than the cache size  $N$ , subsequent tokens could get in and fill the cache. We discard the original KV states of the prefilling tokens and maintain the compressed KV states. They will be concatenated with the KV states of the incoming tokens and compressed together when the cache is filled again. Tokens that appear earlier in the sequence undergo more iterations of compression as the context window expands, whereas less compression will be performed on the more recent tokens. With the iterative FreqKV, the KV cache size is not fixed and is reduced below the context window size during decoding. Since the compression is only performed when the sum of cached KV and incoming tokens reaches the preset size, the computation overhead of the compression could be negligible. For example, with the context size of 4096 and the retaining size of 2048, compression is performed every 2048 tokens for contexts exceeding the original window.

Recent work has found the phenomenon of attention sinks that LLMs tend to assign high attention scores to initial tokens [26, 12]. Therefore, we maintain these initial tokens uncompressed in the cache and only compress tokens that come after them.

During training and the prefilling stage of inference, the whole sentence is tokenized and fed into the model. The attention is computed chunk-wise interleaved with the compression operation. After each compression,  $N - L - S$  incoming tokens are regarded as a chunk and fill the cache, with  $S$  sink

tokens uncompressed. As shown in Figure 2 (b), the incoming tokens in each chunk can not attend to the subsequent tokens. The newly incoming token  $x_M$  will attend to  $S$  sink tokens,  $L$  compressed “tokens”,  $M - N$  previous incoming tokens, and  $x_M$  itself. The calculation of attention in Equation 9 can be reformulated as follows:

$$\tilde{\mathcal{A}}(S, N, L, M) = \text{Softmax} \left( \frac{q_M [K_{0:S-1} \oplus \tilde{K}_{0:L-1}^{S:N-1} \oplus K_{N:M}]^T}{\sqrt{d}} \right) \cdot [V_{0:S-1} \oplus \tilde{V}_{0:L-1}^{S:N-1} \oplus V_{N:M}]. \quad (10)$$

It should be noted that key states in LLMs are often equipped with position embeddings like RoPE [21]. In FreqKV, key states are compressed and cached before applying RoPE. The cached key states are encoded with RoPE when conducting self-attention. They are allocated with position indices within the cache rather than the original sequence, which results in the context window extension without requiring position extrapolation or interpolation. Compressing key states with RoPE is explored in Appendix B.

## 5 Experiments

### 5.1 Implementation

We conduct experiments on long context language modeling and understanding tasks with LLaMA-2-7b [22] and LLaMA-3-8b [1]. We maintain  $S = 4$  sink tokens uncompressed. The retaining ratio  $\gamma$  in compression is set to 0.5. The preset context window size of LLaMA-2 is 4096, which is also the maximum KV cache size  $N$ . Therefore, the retaining size during each compression is  $L = \gamma \cdot (N - S) = 2046$ . As long as the cache size reaches its capacity of 4096, the 4092 states since the 5-th state in the cache will be compressed into 2046 states. The context size of LLaMA-3 is 8192. It is equipped with GQA (Grouped-Query Attention), which means it has a lower proportion of parameters for attention modules than LLaMA-2-Base/Chat-7b (Multi-Head Attention, MHA).

Minimal training is introduced to adapt models to this frequency-domain compression method. For long context language modeling, we fine-tune LLaMA-2-base on the RedPajama [8] pre-training dataset, extending the context window from 4K to 8K, 16K, and 32K. Perplexity (PPL) evaluation is conducted on PG-19 [20] and Proof-pile [2]. For long context understanding, the instruction following dataset LongAlpaca [7] is used for the supervised fine-tuning (SFT) of LLaMA-2-chat and LLaMA-3-instruct. The context window is extended from 4K to 8K, and from 8K to 16K respectively. Models are evaluated on LongBench [3] and Needle-in-a-Haystack [10]. Details of training settings are summarized in Appendix C.

### 5.2 Long Context Language Modeling

We use FreqKV to train LLaMA-2-base-7b on RedPajama with lengths of 8192, 16384, and 32768. Perplexity is measured on test sets of the book corpus dataset PG-19 and the Arxiv math dataset Proof-pile with the evaluation sliding window of 256. We compare our method with other baselines including full fine-tuning (Full FT), LongLoRA [7], and LoCoCo [5]. While Full FT and LongLoRA leverage full KV cache during inference, LoCoCo, and our FreqKV use compressed cache.

PPL scores on different evaluation context lengths are reported in Table 1. While both of LongLoRA and LoCoCo sacrifice performance within the original context length (2K and 4K), FreqKV almost has no performance degradation. Even with the training length of 8K, FreqKV performs comparably to LongLoRA with the training length of 32K. It also outperforms LoCoCo on the extended context length as well as the shorter lengths.

It can be noticed that FreqKV falls behind LongLoRA on Proof-pile at longer context lengths. Proof-pile consists of a diverse set of mathematical texts, including both informal and formal sources, making it particularly challenging for models using compressed caches to predict the next token. In contrast, LongLoRA retains the full KV cache, which naturally benefits next-token prediction in such structured domains. However, the performance of FreqKV does not deteriorate as the context length increases. Our compressed cache method even surpasses Full FT and LongLoRA on PG-19.

Furthermore, we evaluate the performance of FreqKV at longer lengths as shown in Figure 4. With the training length of 8K, it effectively extends the context window to 64K, which is 16 times larger than the original size.

Table 1: Perplexity evaluation on the test sets of PG-19 and Proof-pile. The superscript “\*” means that we reproduce LoCoCo following their official code for evaluation. The results of full fine-tuning and LongLoRA are reported from [7].

Training Length	Method	Inference Cache	Evaluation Context Length				
			2048	4096	8192	16384	32768
PG-19							
8192	Full FT	Full	7.55	7.21	6.98	-	-
	LongLoRA	Full	7.70	7.35	7.14	-	-
	LoCoCo*	Compressed	8.15	8.08	7.27	-	-
	FreqKV	Compressed	7.45	7.12	7.04	7.02	7.02
16384	LongLoRA	Full	7.65	7.28	7.02	6.86	-
	FreqKV	Compressed	7.46	7.13	7.03	6.99	6.98
32768	LongLoRA	Full	8.29	7.83	7.54	7.35	7.22
	FreqKV	Compressed	7.47	7.14	7.04	7.00	6.98
Proof-pile							
8192	Full FT	Full	3.14	2.85	2.66	-	-
	LongLoRA	Full	3.20	2.91	2.72	-	-
	LoCoCo*	Compressed	3.40	3.20	2.88	-	-
	FreqKV	Compressed	3.15	2.88	2.79	2.76	2.75
16384	LongLoRA	Full	3.17	2.87	2.66	2.51	-
	FreqKV	Compressed	3.15	2.88	2.78	2.74	2.73
32768	LongLoRA	Full	3.35	3.01	2.78	2.61	2.50
	FreqKV	Compressed	3.16	2.89	2.78	2.74	2.72

### 5.3 Long Context Understanding

To further validate the performance on downstream tasks, we use FreqKV to extend the context window of LLaMA-2-chat-7b from 4K to 8K and LLaMA-3-instruct-8b from 8K to 16K. Models are evaluated on the long context understanding benchmark LongBench [3] and Needle-in-a-Haystack [10].

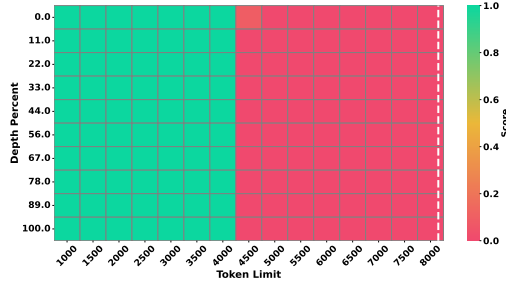
**LongBench.** Scores on the 5 categories of LongBench are reported in Table 2. FreqKV consistently improves the performance of LLaMA-2-chat and LLaMA-3-instruct across a majority of these tasks. We compare our method with different KV compression strategies, including LM-Infinite [12], LongHeads [18], SnapKV [17] and PyramidKV [6]. Most baselines use LLaMA-2-chat-7b as their backbone. The retaining ratio is set to 0.5. FreqKV achieves SOTA (state-of-the-art) on 10 long context understanding tasks for LLaMA-2 and 8 tasks for LLaMA-3.

**Needle-in-a-Haystack.** The Needle-in-a-Haystack results are illustrated in Figure 3. FreqKV performs well in extending the context window of LLaMA-2 and LLaMA-3. In contrast, PyramidKV [6] fails beyond the original window boundary. This is because it merely compresses the KV cache at the first decoding step. Out-of-bound position embeddings are used and it prunes tokens after calculating attention weights. Consequently, those unseen positions lead to the performance collapse.

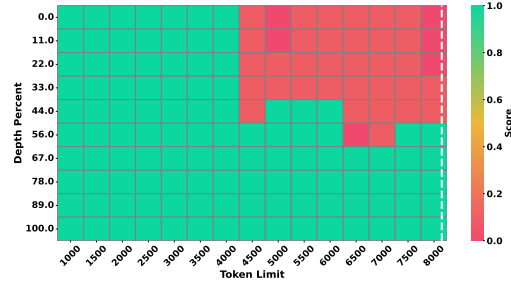
To demonstrate the effectiveness of our compression operation, a variant method Dropping is also implemented for comparison as in Figure 3b. Instead of compressing in the frequency domain, Dropping retains the most recent tokens like StreamingLLM [26]. It shares the same training settings as FreqKV. While Dropping suffers from the permanent loss of earlier tokens, FreqKV could retrieve information from a specific sentence (the “needle”) hidden within a document (the “haystack”) and achieve a better performance.

Table 2: Scores of different KV compression methods on LongBench. The superscript “\*” means that we reproduce SnapKV and PyramidKV following their official codes for evaluation. The results of LM-Infinite and LongHeads are reported from [18].

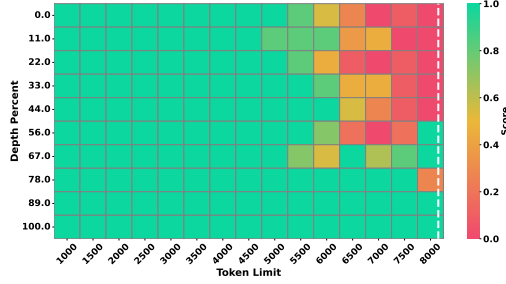
Method	Single-Document QA			Multi-Document QA			Summarization			Few-shot Learning			Code	
	NtrvQA	Qasper	MF-en	HotpotQA	2WikiMQA	Musique	GovReport	QMSum	MultiNews	TREC	TriviaQA	SAMSum	LCC	RB-P
LLaMA2-chat	18.7	19.2	<b>36.8</b>	25.4	32.8	9.4	27.3	20.8	25.8	61.5	77.8	40.7	52.4	43.8
+LM-Infinite	0.00	18.57	25.33	27.34	31.96	7.76	11.30	2.99	8.72	32.50	29.22	13.82	34.19	24.55
+LongHeads	11.61	22.98	23.76	31.28	24.10	8.87	25.36	20.24	16.18	50.67	79.98	36.74	53.85	44.22
+SnapKV*	17.91	22.9	<b>35.3</b>	26.03	28.21	8.77	24.99	20.94	25.92	<b>64.0</b>	83.36	41.0	<b>60.83</b>	55.14
+PyramidKV*	17.36	<b>23.58</b>	34.89	26.28	28.39	9.17	24.95	20.9	26.04	<b>64.0</b>	83.36	40.92	60.68	55.17
+FreqKV	<b>20.41</b>	21.05	31.2	<b>34.54</b>	<b>34.78</b>	<b>14.47</b>	<b>25.51</b>	<b>21.81</b>	<b>26.9</b>	56.0	<b>84.09</b>	<b>41.53</b>	58.99	<b>58.65</b>
LLaMA3-instruct	<b>22.52</b>	31.83	41.04	44.14	36.68	<b>24.05</b>	28.87	23.25	26.46	<b>75.5</b>	90.23	42.09	56.7	51.84
+PyramidKV*	22.27	31.93	41.03	44.79	36.56	23.86	28.77	23.14	26.62	74.5	<b>90.25</b>	<b>42.53</b>	59.11	<b>53.33</b>
+FreqKV	22.18	<b>42.43</b>	<b>44.19</b>	<b>46.63</b>	<b>40.24</b>	19.57	<b>30.48</b>	<b>23.3</b>	<b>28.53</b>	69.5	88.32	41.73	<b>60.41</b>	51.0



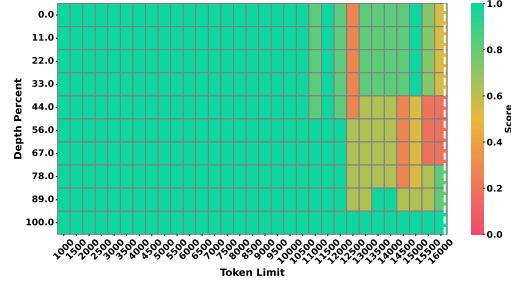
(a) Results of PyramidKV on LLaMA-2. The average accuracy is 46.7%.



(b) Results of Dropping on LLaMA-2. The average accuracy is 75.5%.



(c) Results of FreqKV on LLaMA-2. The average accuracy is 84.2%.



(d) Results of FreqKV on LLaMA-3. The average accuracy is 90.7%.

Figure 3: The Needle-in-a-Haystack results, with the x-axis representing the document length (“haystack”) ranging from 1K to 8K tokens for LLaMA-2-chat-7b and 1K to 16K tokens for LLaMA-3-instruct-8b, and the y-axis showing the position of the “needle” (a short sentence) within the document.

## 6 Analysis

### 6.1 Retaining Ratio

We train LLaMA-2-7b on RedPajama [8] with different retaining ratios. The training length is 8K. Models are evaluated on the validation set of PG-19 with the evaluation length ranging from 2K to 64K.

The performance of FreqKV with different retaining ratios is presented in Figure 4. FreqKV performs better with more frequency components retained. Employing an iterative compression manner, less



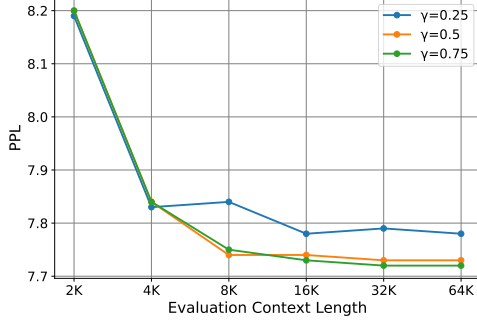


Figure 4: Perplexity evaluation on the validation set of PG-19 with different retaining ratios.

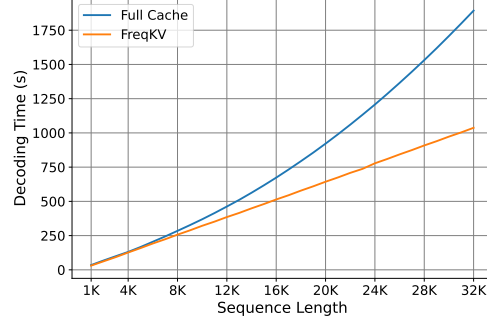


Figure 5: Decoding time with the full cache and FreqKV on the increasing sequence length.

Table 3: The decoding latency (seconds) of FreqKV and Dropping on LLaMA-2-7b with the increasing sequence length. The difference between FreqKV and Dropping shows the compression latency introduced by FreqKV.

Models	4K	8K	16K	24K	32K
Compression Times	0	3	7	11	15
Dropping	123.78 $\pm$ 1.46	253.32 $\pm$ 5.76	506.60 $\pm$ 5.11	760.46 $\pm$ 7.15	1022.50 $\pm$ 18.83
FreqKV	124.34 $\pm$ 1.80	252.75 $\pm$ 3.55	507.61 $\pm$ 5.44	764.82 $\pm$ 9.72	1029.00 $\pm$ 19.97

compressions are performed on the more recent tokens by FreqKV, which benefits long context language modeling. It consistently achieves low perplexity as the evaluation context length grows from 2K to 64K, far exceeding the training length.

## 6.2 Decoding Latency

FreqKV performs compressions on-the-fly during decoding. We compare the decoding time required by LLaMA-2-7b with the full cache and our FreqKV when the sequence length increases. As shown in Figure 5, the decoding time starts to diverge at the length of 4K. While the full cache utilization leads to a quadratic growth in decoding time, the decoding time of FreqKV increases approximately linearly with a negligible time spent on compression, showcasing its efficiency.

Furthermore, we measure the decoding latency of FreqKV and Dropping with the increasing length. Dropping removes the earliest tokens instead of compression in the frequency domain. The difference in the decoding time between the two methods shows the latency of compression. The sink size is set to 4 and the retaining ratio is 0.5. Table 3 reports the average decoding time (seconds) over five runs, along with standard deviations. It can be observed that the additional latency (6.5s) introduced by FreqKV accounts for only 0.64% of the total decoding time at 32K tokens. Further analysis for the compression overhead is provided in Appendix D.

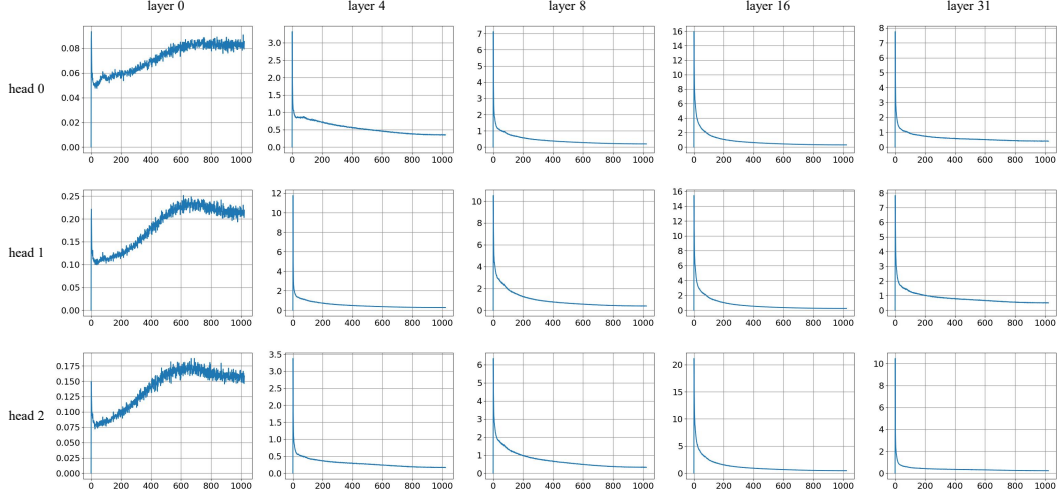
## 7 Conclusion

In this paper, we introduce FreqKV to compress KV states iteratively in the frequency domain for LLMs. We exploit the energy concentration of KV states in the frequency domain within the decoder layers. Specifically, we filter out the high-frequency components that are of low magnitude and retain the low-frequency components for compression. The KV cache is compressed in the frequency domain without introducing additional compression modules. Iteratively compressing the KV cache, FreqKV could extend the context window efficiently for LLMs. With minimal training of low-rank adaption, LLMs learn to leverage the compressed KV cache. Through extensive experiments and analysis on long context modeling and understanding, FreqKV demonstrates its efficiency and effectiveness in context extension.

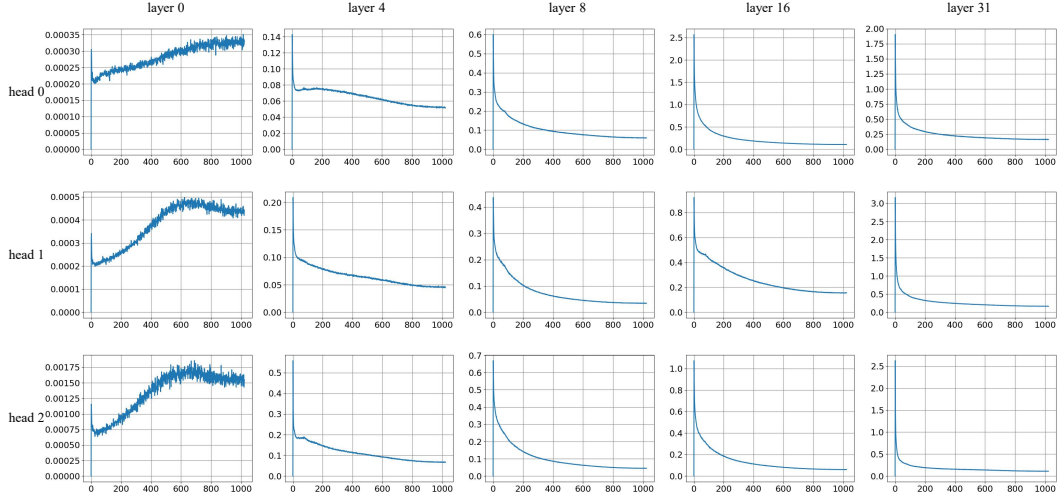
## References

- [1] AI@Meta. Llama 3 model card. 2024. URL [https://github.com/meta-llama/llama3/blob/main/MODEL\\_CARD.md](https://github.com/meta-llama/llama3/blob/main/MODEL_CARD.md).
- [2] Zhangir Azerbayev, Edward Ayers, and Bartosz Piotrowski. Proof-pile, 2022. URL <https://huggingface.co/datasets/hoskinson-center/proof-pile>.
- [3] Yushi Bai, Xin Lv, Jiajie Zhang, Hongchang Lyu, Jiankai Tang, Zhidian Huang, Zhengxiao Du, Xiao Liu, Aohan Zeng, Lei Hou, Yuxiao Dong, Jie Tang, and Juanzi Li. Longbench: A bilingual, multitask benchmark for long context understanding, 2024. URL <https://arxiv.org/abs/2308.14508>.
- [4] Iz Beltagy, Matthew E. Peters, and Arman Cohan. Longformer: The long-document transformer, 2020. URL <https://arxiv.org/abs/2004.05150>.
- [5] Ruisi Cai, Yuandong Tian, Zhangyang Wang, and Beidi Chen. Lococo: Dropping in convolutions for long context compression, 2024a. URL <https://arxiv.org/abs/2406.05317>.
- [6] Zefan Cai., Yichi Zhang, Bofei Gao, Yuliang Liu, Tianyu Liu, Keming Lu, Wayne Xiong, Yue Dong, Baobao Chang, Junjie Hu, and Wen Xiao. Pyramidkv: Dynamic kv cache compression based on pyramidal information funneling, 2024b. URL <https://arxiv.org/abs/2406.02069>.
- [7] Yukang Chen, Shengju Qian, Haotian Tang, Xin Lai, Zhijian Liu, Song Han, and Jiaya Jia. Longlora: Efficient fine-tuning of long-context large language models, 2024. URL <https://arxiv.org/abs/2309.12307>.
- [8] Together Computer. Redpajama: an open dataset for training large language models, 2023. URL <https://github.com/togethercomputer/RedPajama-Data>.
- [9] Tri Dao. Flashattention-2: Faster attention with better parallelism and work partitioning, 2023. URL <https://arxiv.org/abs/2307.08691>.
- [10] gkamradt. Llmtest needle in a haystack - pressure testing llms. [https://github.com/gkamradt/LLMTest\\_NeedleInAHaystack](https://github.com/gkamradt/LLMTest_NeedleInAHaystack), 2023.
- [11] Lionel Gueguen, Alex Sergeev, Ben Kadlec, Rosanne Liu, and Jason Yosinski. Faster neural networks straight from jpeg. In S. Bengio, H. Wallach, H. Larochelle, K. Grauman, N. Cesa-Bianchi, and R. Garnett, editors, *Advances in Neural Information Processing Systems*, volume 31. Curran Associates, Inc., 2018. URL [https://proceedings.neurips.cc/paper\\_files/paper/2018/file/7af6266cc52234b5aa339b16695f7fc4-Paper.pdf](https://proceedings.neurips.cc/paper_files/paper/2018/file/7af6266cc52234b5aa339b16695f7fc4-Paper.pdf).
- [12] Chi Han, Qifan Wang, Hao Peng, Wenhan Xiong, Yu Chen, Heng Ji, and Sinong Wang. Lm-infinite: Zero-shot extreme length generalization for large language models, 2024. URL <https://arxiv.org/abs/2308.16137>.
- [13] Ziwei He, Meng Yang, Minwei Feng, Jingcheng Yin, Xinbing Wang, Jingwen Leng, and Zhouhan Lin. Fourier transformer: Fast long range modeling by removing sequence redundancy with fft operator. In *Findings of the Association for Computational Linguistics: ACL 2023*, page 8954–8966. Association for Computational Linguistics, 2023. doi: 10.18653/v1/2023.findings-acl.570. URL <http://dx.doi.org/10.18653/v1/2023.findings-acl.570>.
- [14] Karl Moritz Hermann, Tomáš Kočiský, Edward Grefenstette, Lasse Espeholt, Will Kay, Mustafa Suleyman, and Phil Blunsom. Teaching machines to read and comprehend, 2015.
- [15] Edward J. Hu, Yelong Shen, Phillip Wallis, Zeyuan Allen-Zhu, Yanzhi Li, Shean Wang, Lu Wang, and Weizhu Chen. Lora: Low-rank adaptation of large language models, 2021. URL <https://arxiv.org/abs/2106.09685>.
- [16] James Lee-Thorp, Joshua Ainslie, Ilya Eckstein, and Santiago Ontanon. Fnet: Mixing tokens with fourier transforms, 2022. URL <https://arxiv.org/abs/2105.03824>.

- [17] Yuhong Li, Yingbing Huang, Bowen Yang, Bharat Venkitesh, Acyr Locatelli, Hanchen Ye, Tianle Cai, Patrick Lewis, and Deming Chen. Snapkv: Llm knows what you are looking for before generation, 2024. URL <https://arxiv.org/abs/2404.14469>.
- [18] Yi Lu, Xin Zhou, Wei He, Jun Zhao, Tao Ji, Tao Gui, Qi Zhang, and Xuanjing Huang. Longheads: Multi-head attention is secretly a long context processor, 2024. URL <https://arxiv.org/abs/2402.10685>.
- [19] Amirkeivan Mohtashami and Martin Jaggi. Landmark attention: Random-access infinite context length for transformers, 2023. URL <https://arxiv.org/abs/2305.16300>.
- [20] Jack W. Rae, Anna Potapenko, Siddhant M. Jayakumar, and Timothy P. Lillicrap. Compressive transformers for long-range sequence modelling, 2019. URL <https://arxiv.org/abs/1911.05507>.
- [21] Jianlin Su, Yu Lu, Shengfeng Pan, Ahmed Murtadha, Bo Wen, and Yunfeng Liu. Roformer: Enhanced transformer with rotary position embedding, 2023. URL <https://arxiv.org/abs/2104.09864>.
- [22] Hugo Touvron, Louis Martin, Kevin Stone, Peter Albert, Amjad Almahairi, Yasmine Babaei, Nikolay Bashlykov, Soumya Batra, Prajjwal Bhargava, Shruti Bhosale, Dan Bikel, Lukas Blecher, Cristian Canton Ferrer, Moya Chen, Guillem Cucurull, David Esiobu, Jude Fernandes, Jeremy Fu, Wenyin Fu, Brian Fuller, Cynthia Gao, Vedanuj Goswami, Naman Goyal, Anthony Hartshorn, Saghar Hosseini, Rui Hou, Hakan Inan, Marcin Kardas, Viktor Kerkez, Madian Khabsa, Isabel Kloumann, Artem Korenev, Punit Singh Koura, Marie-Anne Lachaux, Thibaut Lavril, Jenya Lee, Diana Liskovich, Yinghai Lu, Yuning Mao, Xavier Martinet, Todor Mihaylov, Pushkar Mishra, Igor Molybog, Yixin Nie, Andrew Poulton, Jeremy Reizenstein, Rashi Rungta, Kalyan Saladi, Alan Schelten, Ruan Silva, Eric Michael Smith, Ranjan Subramanian, Xiaoqing Ellen Tan, Binh Tang, Ross Taylor, Adina Williams, Jian Xiang Kuan, Puxin Xu, Zheng Yan, Iliyan Zarov, Yuchen Zhang, Angela Fan, Melanie Kambadur, Sharan Narang, Aurelien Rodriguez, Robert Stojnic, Sergey Edunov, and Thomas Scialom. Llama 2: Open foundation and fine-tuned chat models, 2023. URL <https://arxiv.org/abs/2307.09288>.
- [23] Ashish Vaswani, Noam Shazeer, Niki Parmar, Jakob Uszkoreit, Llion Jones, Aidan N. Gomez, Lukasz Kaiser, and Illia Polosukhin. Attention is all you need, 2023. URL <https://arxiv.org/abs/1706.03762>.
- [24] Zhongwei Wan, Xinjian Wu, Yu Zhang, Yi Xin, Chaofan Tao, Zhihong Zhu, Xin Wang, Siqi Luo, Jing Xiong, and Mi Zhang. D2o: Dynamic discriminative operations for efficient generative inference of large language models, 2024. URL <https://arxiv.org/abs/2406.13035>.
- [25] Zheng Wang, Boxiao Jin, Zhongzhi Yu, and Minjia Zhang. Model tells you where to merge: Adaptive kv cache merging for llms on long-context tasks, 2024. URL <https://arxiv.org/abs/2407.08454>.
- [26] Guangxuan Xiao, Yuandong Tian, Beidi Chen, Song Han, and Mike Lewis. Efficient streaming language models with attention sinks, 2024. URL <https://arxiv.org/abs/2309.17453>.
- [27] Kai Xu, Minghai Qin, Fei Sun, Yuhao Wang, Yen-Kuang Chen, and Fengbo Ren. Learning in the frequency domain, 2020. URL <https://arxiv.org/abs/2002.12416>.
- [28] Peitian Zhang, Zheng Liu, Shitao Xiao, Ninglu Shao, Qiwei Ye, and Zhicheng Dou. Soaring from 4k to 400k: Extending llm’s context with activation beacon, 2024. URL <https://arxiv.org/abs/2401.03462>.
- [29] Yuxin Zhang, Yuxuan Du, Gen Luo, Yunshan Zhong, Zhenyu Zhang, Shiwei Liu, and Rongrong Ji. CaM: Cache merging for memory-efficient LLMs inference. In Ruslan Salakhutdinov, Zico Kolter, Katherine Heller, Adrian Weller, Nuria Oliver, Jonathan Scarlett, and Felix Berkenkamp, editors, *Proceedings of the 41st International Conference on Machine Learning*, volume 235 of *Proceedings of Machine Learning Research*, pages 58840–58850. PMLR, 21–27 Jul 2024. URL <https://proceedings.mlr.press/v235/zhang24n.html>.



(a) The average power spectrums of key states.



(b) The average power spectrums of value states.

Figure 6: The average power spectrums of key states and value states in different heads of Llama-2-7b.

## A Head-wise Analysis of Power Spectrums

We explore the power spectrum distribution of key states and value states in different attention heads of LLaMA-2-7b as shown in Figure 6. Although values of power spectrums vary in different heads, their distribution exhibits similar patterns. They have a consistent tendency to aggregate energy in the low-frequency components along the decoding procedure. It could be promising to study specific differences and associations in different heads or other modules.

## B Compressing Key States with RoPE

We further investigate to compress key states after applying RoPE. Power spectrums of key states with RoPE are provided in Figure 7. Components of certain frequencies are filtered out by RoPE.

We train LLaMA-2-7b on RedPajama with the variant method that key states are compressed after applying RoPE. The training length is 8K. Models are evaluated on the test set of PG-19 and Proofpile. The results in Table 4 demonstrate that the variant suffers from performance degradation, which is probably due to the usage of position embeddings out of the original window. In contrast, FreqKV

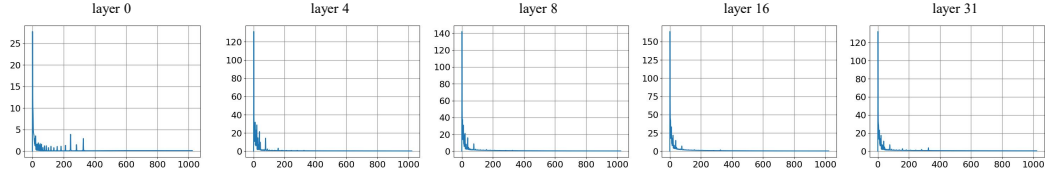


Figure 7: The average power spectrums of key states with RoPE.

compresses and caches key states before applying RoPE. Therefore, they are allocated with position indices within the original window rather than the lengthy sequence, which results in the context window extension with no need of using out-of-bound position embeddings.

Table 4: Perplexity evaluation on the test sets of PG-19 and Proof-pile. “Variant” stands for FreqKV with key states compressed after applying RoPE.

Dataset	Method	Evaluation Context Length		
		2048	4096	8192
<i>PG-19</i>	Full FT	7.55	7.21	6.98
	FreqKV	7.45	7.12	7.04
	Variant	7.53	7.19	7.13
<i>Proof-pile</i>	Full FT	3.14	2.85	2.66
	FreqKV	3.15	2.88	2.79
	Variant	3.16	2.88	2.80

## C Training settings

For long context language modeling, we fine-tune LLaMA-2-base on the RedPajama [8] pre-training dataset for 1000 steps. For long context understanding, we SFT LLaMA-2-chat and LLaMA-3-instruct on the instruction following dataset LongAlpaca [7] for 5 epochs, which consists of 6.28K long-context QA samples.

The total batch size ( $GPU\_number \times Batch\_size\_per\_device \times Gradient\_accumulation\_steps$ ) is 64. The learning rate increases linearly from  $1e-6$  to  $2e-5$  with 20 warm-up steps and remains constant in the following steps. The rank used in the LoRA [15] fine-tuning is set to 8. Following LongLoRA [7], the embedding and normalization layers are learnable during training. All the experiments are conducted on ADA6000 and H100 GPUs. Moreover, we equip our method with FlashAttention-2 [9] for further acceleration and memory saving.

## D Compression Overhead

We conduct further studies on the compression overhead of FreqKV. As introduced in Section 4.3, chunk-wise attention is performed for the prefilling tokens. The size of the attention matrix in each chunk is  $(N - L - S) \cdot N$  except for the last few tokens. Therefore, the computational cost of self-attention grows approximately linearly with the input length like sliding window attention [4].

We use torchprofile<sup>2</sup> to count the number of Floating Point Operations (FLOPs) with input sequences of different lengths for LLaMA-2-7b. We calculate FLOPs for the model with the original attention which leverages full KV states, and with FreqKV with the retaining ratio of 0.5. To quantify the compression overhead, we have measured FLOPs of the Dropping, which retains the most recent tokens instead of compressing in the frequency domain. It shares the same sink size and retaining size as FreqKV. The difference in FLOPs between the two methods shows the overhead of compression.

<sup>2</sup><https://github.com/zhijian-liu/torchprofile>

The statistics are given in Table 5. The compression times of FreqKV with different context lengths are also reported in the table. It shows that the computation overhead of our compression process grows less than 0.5% even with a length of 32K, which could be negligible. FreqKV reduces more FLOPs as the input length grows from 4K to 32K compared to Full KV. This is because the compression is performed every  $N - L - S$  tokens with the complexity of  $O(N \log N)$ , which is negligible compared to the quadratic self-attention.

Table 5: FLOPs (TFLOPs) with input sequences of different lengths. Experiments are conducted on the ADA6000 GPU of 48GB, where full KV of 12K tokens with float16 will cause an OOM (Out-of-Memory) issue. The difference between FreqKV and Dropping shows the computation overhead of compression.

<b>Models</b>	<b>4K</b>	<b>8K</b>	<b>12K</b>	<b>16K</b>	<b>32K</b>
Full KV	62.93	143.46	OOM	OOM	OOM
Dropping	62.93	125.86	188.79	251.72	503.43
FreqKV	62.93	125.90	188.85	251.81	503.63
Compression Overhead	0 (0%)	0.039 (0.031%)	0.064 (0.034%)	0.090 (0.036%)	0.193 (0.038%)
Compression Times	0	3	5	7	15